Effect of Wall Curvature on Curved Duct Flows

홍승규, 허기훈, 이광섭
국방과학연구소

Abstract

Effect of wall curvature on flow characteristics is studied for mildly and strongly curved duct flows. The ducts are S-shaped, and the flow is partially blocked at the rear of the downstream. The presence of blockage in combination with curvature generates secondary flows on the concave surface; the magnitude of the secondary flow being dependent on the degree of wall curvature. Objectives are to compare the flow structures for mild and strong cases and to illuminate the changes in flow structure as the flow turns. Sensitivity on numerical solutions due to different inflow boundary conditions is also examined.

1. INTRODUCTION

Tunnels, pipes, inlets and ducts, either curved or straight, are common encounters in our everyday lives. Their role is in general to change the direction of the flow or re-direct it. The inlets, in particular, when attached to the airplane feed the upstream flow to the engine blades in a desired manner. When the speed of the vehicle approaches transonic, the presence of hub absorbs the direct impact of the external flow on the engine blades by first partially blocking the oncoming flow and then supplies stable and even flow onto the engine face.

In the present study, two arbitrarily curved ducts are constructed with different wall curvatures. Primary aim is to investigate the effect of mild and strong curvatures on the flow structures inside the duct flows. Inlet performances are judged by the degree of flow distortion at the engine face and by the loss of total pressure drop. By also making the duct S-shaped, the effect of curvature is neutralized after the curvature changes from convex to concave, or vise versa. In the computation, multiple grids are utilized to avoid the singular line and to accomodate the hub area in a smooth manner which causes least amount of grid skewness. Solutions are then obtained for mildly and strongly curved duct flows.

2. PROBLEM DESCRIPTION

Two ducts are subject to a uniform flow at a sea level condition. The ducts are mildly and strongly curved with the L/D=5.0 and 2.5, respectively, where L is the length of the duct and D, the diameter of it. Dependence of separation zones on the curvature is of interest. In order to see the sensitivity of the inflow conditions, both fixed inflow condition and a characteristic inflow condition based on constant total enthalpy condition are employed and their results are compared.

3. NUMERICAL METHOD

The basic numerical algorithm follows Roe-averaged flux-difference splitting (RFDS) method[1,2], although many ideas are originated from flux-vector splitting formulations of Warming and Beam[3], Pulliam and Steger[4], Pulliam and Chaussee[5], from conservative supra-characteristics method (CSCM) of Lombard et al.[6-9], characteristic flux-difference splitting (CFDS) method of Yang et al.[10,11], among many

others.

The governing Navier-Stokes equations employed in the generalized coordinate system, $(\xi, \eta, \phi,)$ are expressed for the conservative variable vector as

$$J^{-1}\frac{\partial q}{\partial t} + \tilde{\xi}_x\frac{\partial}{\partial \xi}(\hat{F} + \hat{F}_v) + \tilde{\eta}_x\frac{\partial}{\partial \eta}(\hat{G} + \hat{G}_v) + \tilde{\phi}_x\frac{\partial}{\partial \phi}(\hat{H} + \hat{H}_v) = 0 \tag{1}$$

where $\hat{F}$, $\hat{G}$, and $\hat{H}$ are inviscid flux vectors, and $\hat{F}_v$, $\hat{G}_v$, $\hat{H}_v$ are viscous flux vectors. Also, $\tilde{\xi}_x = \xi_x \cdot J^{-1} = \xi_x / J$, etc. As before, the inviscid fluxes, are linearized for upwind discretizations by

$$\Delta_\xi F = \tilde{A}\Delta q = (\tilde{A}^+ + \tilde{A}^-)\Delta q$$

and $$\tilde{A}^\pm = M T \Lambda^\pm T^{-1} M_t^{-1} \tag{2}$$

yielding

$$J^{-1}\delta q + \tilde{A}^+\nabla_\xi q + \tilde{A}^-\Delta_\xi q + \tilde{B}^+\nabla_\eta q + \tilde{B}^-\Delta_\eta q + \tilde{C}^+\nabla_\phi q + \tilde{C}^-\Delta_\phi q + (\text{viscous terms}) = 0 \tag{3}$$

The matrix $\tilde{B}^\pm$ is the same as $\tilde{A}^\pm$ except that ξ in $\tilde{A}^\pm$ is replaced by η, and the matrix $\tilde{C}^\pm$ takes ϕ instead of ξ in $\tilde{A}^\pm$. Also the viscous flux vectors associated with ξ, η and ϕ directions, respectively, can be related to the conservative vector q via

$$\hat{F}_v = A_v\Delta_\xi q \quad \hat{G}_v = B_v\Delta_\eta q \quad \hat{H}_v = C_v\Delta_\phi q \tag{4}$$

For simplicity and practical purpose, ξ-direction viscous flux is neglected, and viscous coefficient matrices B_v and C_v are retained in the current formulation. Upwind flux-difference splitting for the inviscid fluxes and second-order central differencing for the viscous fluxes are then applied for discretizations. Presently, solutions are updated from q^n to q^{n+1} via implicit approximation in (ξ, η, ϕ) -plane and symmetric Gauss-Seidel relaxation for ξ-direction.

Choice of proper boundary conditions is crucial for not only fast convergence but also accuracy of solutions. Application of characteristic boundary procedure is based upon a realization that there are five characteristics associated with the convective part of the Navier-Stokes equations. For subsonic inflow boundary, we have either fixed the flows or utilized a characteristic condition that the total enthalpy is constant, i.e. $\partial H / \partial t = 0$, through a modification in the 4^{th} row of T^{-1} by

$$\left[-\frac{1}{\gamma P}, u, v, w, \gamma \right],$$

to replace the $\delta P^+ - equation$ at the left.

For subsonic outflow boundary, one usually incorporates a condition that the pressure is constant, i.e. $\partial p / \partial t = 0$, through a modification in the 5^{th} row of T^{-1} by

$$\left[0, 0, 0, 0, \frac{1}{\gamma P} \right],$$

to replace the $\delta P^- - equation$ at the right by

$$\delta \tilde{\tilde{q}} = T^{-1} \delta \tilde{q} = \delta P / \gamma P = 0. \quad (5)$$

At the wall, no-slip condition for velocity and adiabatic condition for temperature are imposed in the direction normal to the wall. In the symmetry plane, values are extrapolated from neighboring planes.

4. RESULTS AND DISCUSSIONS

The two ducts are termed mildly and strongly curved ducts, and the duct domain is divided into three blocks as shown in Fig. 1 for the symmetric half. The grid topology is devised differently for each of the three domains: the rectangular core region denoted as Grid 1 is represented by a rectangular grid and the Grid 2 is a wrap-around grid, and the Grid 3 surrounds the hub. This particular grid set eliminates singularity in the core region and enhances the convergence of solution. The grids with different topologies are overlapped by a grid cell where the two joining grids exchange data at the matching points. The grid consists of (j,k,l)=(11,120,21) for grid 1, (92,27,37) for grid 2, and (30,56,37) for grid 3, totaling 181,788 points.

Computational results obtained on Cray-YMP are presented in the form of Mach contours in the symmetry plane, total pressure contours in the exit plane and velocity vectors in front of hub region. First, Mach contours are shown in Fig. 2 for mildly curved case with fixed inflow at Mach=0.7, in Fig. 3 for the same case with characteristic boundary condition where total enthalpy is assumed given from free-stream value, and in Fig. 4 for strongly curved duct flow with fixed boundary. The two figures, Figs. 2 and 3, are almost identical and computed massflux ratio between the outflow and the inflow yields 99.94% for the fixed case and 99.93% for the constant enthalpy case. At other cases when one incorporates fixed inflow boundary, solutions sometimes jump from the first station to the second station when solutions are updated. This is not the case for Fig. 2, showing smooth development of solutions. Strongly curved flow is thus computed with fixed inflow and Mach contours are given in Fig. 4. Comparison of Figs. 2 and 4 shows the curvature effect on the two flow fields. The flow with strong curvature is accompanied by a larger separation zone where the secondary flow is quite strong.

The amount of flow distortion due to wall curvature can be measured by total pressure at the exit plane. Figure 5 contains total pressure contours for (a) mild and (b) strong flows; the latter case exhibits clearly a severe distortion, which has larger energy loss, due to stronger curvature. The ratio of averaged total pressure between the exit plane and the inflow plane is 0.938 for the mild flow and 0.910 for the strong flow. These numbers are measure of flow recovery after a flow passed through a duct and a indication of how good a duct is designed.

Finally, velocity vectors are compared for the two flow cases in the flow separation zone. A larger flow reversal is observed in the strongly curved case where flow stagnates longer in the upper concave zone, which leads a lower recovery rate for the stronger case than the mild case.

5. CONCLUDING REMARKS

Objectives of present work were to test two different inflow cases for subsonic flow, on the one hand, and to illustrate influence of wall curvature on flow structure in duct flows, on the other.

Emphasis has also been placed on utilizing a multiple grid set which eliminates the grid singularity along the core of the duct flow. The current results show amount of curvature effects on Mach contours, total pressures and flow recovery for the two curved duct flows. Present work is thus shown to provide a computational procedure for designing and analyzing internal duct flows with a modest obstacle.

ACKNOWLEDGEMENTS

Authors express their thanks to computer support group at ADD for allowing us a convenient access to Cray-YMP.

REFERENCES

1. Roe, P. L., "The use of Riemann problem in finite difference schemes," Lecture Notes in Physics, Vol. 141, 1981, pp. 354-359, Berlin, Springer Verlag.

2. Roe, P. L., "Approximate Riemann solvers, parameter vectors and difference scheme," J. of Computational Physics, 43, 1981, pp. 357-372.

3. Warming, R.F. and Beam, R. M.,"On the Construction of Implicit Factored Schemes for Conservation Laws," Computational Fluid Dynamics, SIAM-AMS Proceedings, Vol. 11, 1978, pp.85-127.

4. Pulliam, T. H. and Steger, J. L. "On Implicit Finite Difference Simulations of Three-Dimensional Flows," AIAA-78-10, January 1978.

5. Pulliam, T. H. and Chaussee, D. S., "A Diagonal Form of an Implicit Approximate-Factorization Algorithm,", Journal of Computational Physics, Vol. 39, pp.347-363, 1981.

6. Lombard, C. K., Oliger, J., Yang, J. Y. and Davy, W. C., "Conservative Supra-Characteristics Method for Splitting the Hyperbolic Systems of Gasdynamics with Computed Boundaries for Real and Perfect Gases," AIAA-82-0837, June 1982.

7. Lombard, C. K., Oliger, J., Yang, J. Y. "A Natural Conservative Flux Difference Splitting for the Hyperbolic Systems of Gasdynamics," AIAA-82-0976, June 1982.

8. Lombard, C. K., et al., "Multi-Dimensional Formulation of CSCM - An Upwind Flux Difference Eigenvector Split Method for the Compressible Navier-Stokes Equations", AIAA-83-1895, AIAA 6th CFD Conference, July 1983.

9. Hong, S. K., Bardina, J., Lombard, C. K., Wang, D. and Codding, W., "A Matrix of 3-D Turbulent CFD Solutions for JI Control with Interacting Lateral and Attitude Thrusters,"AIAA 91-2099, Sacramento, June 1991.

10. Yang, J. Y., "A Characteristic Flux Difference Splitting Method for Hyperbolic Systems of Conservation Laws," Ph.D. Thesis, Stanford University, June 1982.

11. Yang. J. Y. and Lombard, C. K., "A Characteristic Flux Difference Splitting for the Hyperbolic Conservation Laws of Inviscid Gasdynamics," AIAA-83-0040, Reno, Jan 1983.

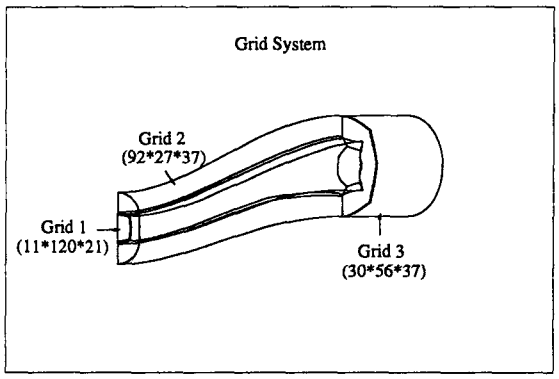

Fig 1. Grid Topology for Duct Flow

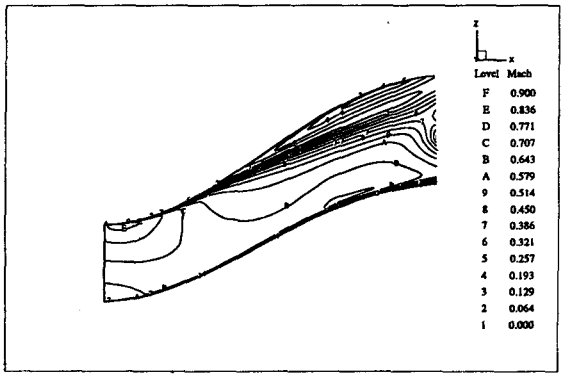

Fig 4. Mach Contours for Strongly Curved Duct (fixed inflow B.C.)

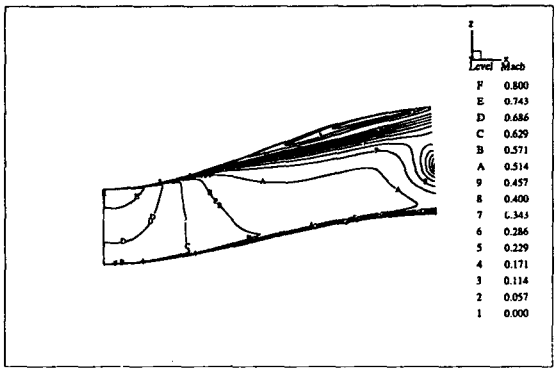

Fig 2. Mach Contours for Mildly Curved Duct (fixed inflow B.C.)

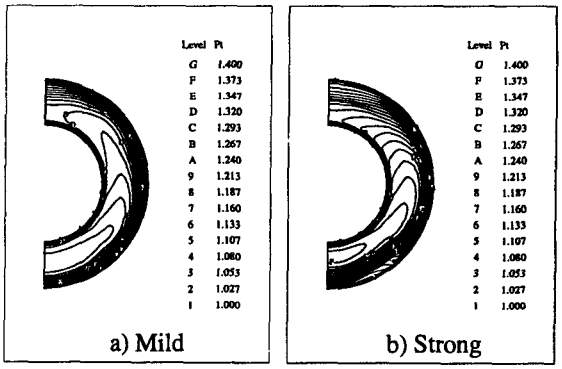

Fig 5. Total Pressure Contours in Exit Planes for a) Mild and b) Strong Cases

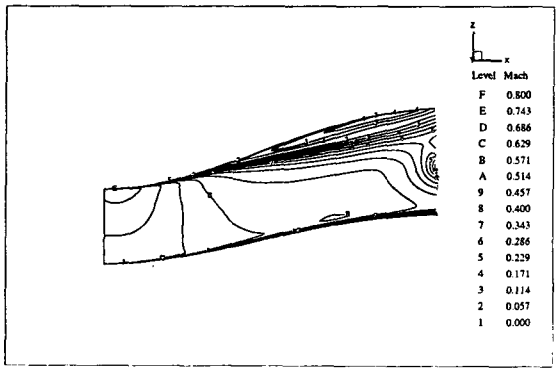

Fig 3. Mach Contours for Mildly Curved Duct (characteristic inflow B.C.)

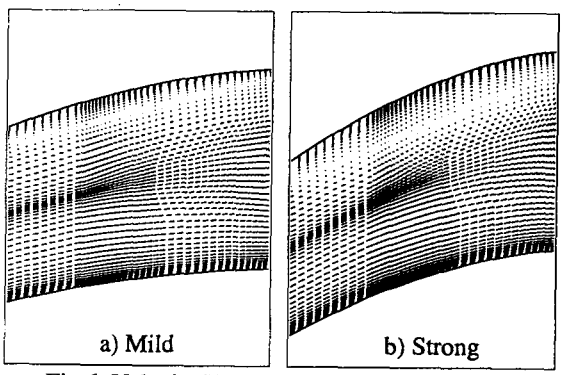

Fig 6. Velocity Vectors in Separation Zones for a) Mild and b) Strong Cases